O'Hair Richard (Orcid ID: 0000-0002-8044-0502)

Manuscript RCM-18-0041:

REVISED Version: 23 March 2018

Unimolecular Reactivity of Organotrifluoroborate Anions, RBF_3^-, and Their Alkali Metal Cluster Ions, $M(RBF_3)_2^-$ (M = Na, K; R = CH_3, CH_3CH_2, $CH_3(CH_2)_3$, $CH_3(CH_2)_5$, c-C_3H_5, C_6H_5, $C_6H_5CH_2$, CH_2CHCH_2, CH_2CH, C_6H_5CO).

Fiona L. B. Bathie,[a] Chris J. Bowen,[b] Craig A. Hutton,[a] and Richard A. J. O'Hair [a]*

(a) School of Chemistry and Bio21 Institute of Molecular Science and Biotechnology, The University of Melbourne, Parkville, Victoria 3010 Australia
(b) Shimadzu Scientific, Bio21 Institute of Molecular Science and Biotechnology, The University of Melbourne, Parkville, Victoria 3010 Australia

*Corresponding author: rohair@unimelb.edu.au

Phone: +613 8344 2452 Fax: +613 9347 5180

Key words: Organotrifluoroborate • Electrospray ionization • Tandem mass spectrometry • Collision-induced dissociation • DFT calculations

Abstract:

Rationale

Potassium organotrifluoroborates RBF_3K are important reagents used in organic synthesis. Although mass spectrometry is commonly used to confirm their molecular formulae, the gas-phase fragmentation reactions of organotrifluoroborates and their alkali metal cluster ions have not been previously reported.

Methods

Negative-ion mode electrospray ionization (ESI) together with collision-induced dissociation (CID) using a triple quadrupole mass spectrometer were used to examine the fragmentation pathways for RBF_3^- (where R = CH_3, CH_3CH_2, $CH_3(CH_2)_3$, $CH_3(CH_2)_5$, c-C_3H_5, C_6H_5, $C_6H_5CH_2$, CH_2CHCH_2, CH_2CH, C_6H_5CO) and $M(RBF_3)_2^-$ (M = Na, K), while density functional theory (DFT) calculations at the M06/def2-TZVP level of theory were used to examine the structures and energies associated with fragmentation reactions for R = Me and Ph.

Results

Upon CID, preferentially elimination of HF occurs for RBF_3^- ions for systems where R = an alkyl anion, whereas R^- formation is favoured when R = a stabilised anion. At higher collision energies loss of F^- and additional HF losses are sometimes observed. Upon CID of $M(RBF_3)_2^-$ formation of RBF_3^- is the preferred pathway with some fluoride transfer observed only when M = Na. The DFT calculated relative thermochemistry for competing fragmentation pathways is consistent with the experiments.

Conclusions

The main fragmentation pathways of RBF_3^- are HF elimination and/or R^- loss. This contrasts with the fragmentation reactions of other organometallate anions, where reductive elimination, beta hydride transfer and bond homolysis are often observed. The presence of fluoride transfer upon CID of Na$(RBF_3)_2^-$ but not K$(RBF_3)_2^-$ is in agreement with the known fluoride affinities of Na^+ and K^+ and can be rationalized by Pearson's HSAB theory.

Running Head: Unimolecular Reactivity of Organotrifluoroborate Anions

1. Introduction:

Organoboron compounds are important substrates used in organic synthesis.[1,2] Amongst the various classes of these reagents, potassium organotrifluoroborates RBF_3K are attractive since they: are air stable solids; can readily be prepared from any boronic acid derivative in high yield for a wide range of organic groups (R = alkyl, aryl, alkenyl, alkynyl etc.); undergo a number of useful reactions including in situ formation of RBF_2 via fluoride abstraction by Lewis acids and transmetallation reactions.[3-5] Although electrospray ionization of these RBF_3K salts has been noted to readily generate organotrifluoroborate anions for HRMS studies,[6] the gas-phase fragmentation reactions of RBF_3^- have not yet been reported. Here we examine the CID reactions of a range of organotrifluoroborates that are representative of various organic groups, R, to establish the competition between loss of the organic anion (eq. 1), loss of fluoride (eq. 2), and loss of HF (eq. 3). Where relevant, we make comparisons to the fragmentation of other classes of organoborates and organometallates. In addition, we examine the fragmentation reactions of alkali metal cluster ions, $M(RBF_3)_2^-$ to probe the competition between formation of RBF_3^- (eq. 4) and fluoride transfer (eq. 5).

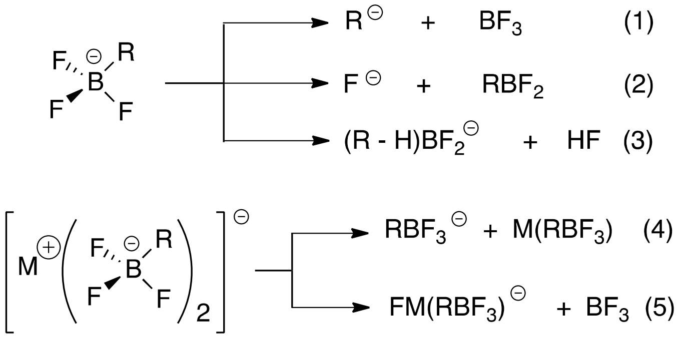

R = Me (CH_3); Et (CH_3CH_2); Bu ($CH_3(CH_2)_3$); Hex ($CH_3(CH_2)_5$); c-Pr (c-C_3H_5); Ph (C_6H_5); $PhCH_2$ ($C_6H_5CH_2$); allyl (CH_2CHCH_2); vinyl (CH_2CH), benzoyl (C_6H_5CO).

Scheme 1: Potential competing fragmentation pathways for organotrifluoroborate anions, RBF_3^-, and their alkali metal cluster ions, $M(RBF_3)_2^-$ together with the systems studied here.

2. Experimental and Theoretical Methods.

2.1 Materials: The following potassium organotrifluoroborates salts, RBF_3K, were sourced from Sigma Aldrich and used without further purification, where R= : CH_3, potassium methyltrifluoroborate, $MeBF_3K$; CH_3CH_2, potassium ethyltrifluoroborate, $EtBF_3K$ (95%); c-C_3H_5, potassium cyclopropyltrifluoroborate, cyclopropyl BF_3K (90-95%); $C_6H_5CH_2$, potassium benzyltrifluoroborate, benzyl BF_3K (95%); CH_2CHCH_2, potassium allyltrifluoroborate, allyl BF_3K (95%); C_6H_5CO, potassium benzoyltrifluoroborate, benzoyl BF_3K. The remaining salts, RBF_3K, were available from a previous study where R= : $CH_3(CH_2)_3$, potassium butyltrifluoroborate, $BuBF_3K$; $CH_3(CH_2)_5$, potassium hexyltrifluoroborate, $HexBF_3K$; C_6H_5, potassium phenyltrifluoroborate, $PhBF_3K$; CH_2CH, potassium vinyltrifluoroborate, $vinBF_3K$.[7]

2.2 Mass spectrometry:

Electrospray ionization mass spectrometry and tandem mass spectrometry experiments (MS/MS analysis) was performed using a Nexera X2 UHPLC System (Shimadzu Corporation, Kyoto, Japan) interfaced with a LCMS-8060 (Shimadzu Corporation, Kyoto, Japan) triple quadrupole mass spectrometer. The UHPLC system was operated in the isocratic, flow injection mode, delivering 250 µL/min of acetonitrile with 5 µL injections of each potassium organotrifluoroborate sample. The dual ion source (DUIS) interface was set for electrospray ionization, operating in the negative mode with the interface parameters optimized to the following conditions: nebulizer gas flow: 2 L/min; heating gas flow: 10 L/min; interface temperature: 300 °C; desolvation line temperature: 250 °C; heat block temperature: 400 °C and interface voltage: 3 kV. The mass spectrometer was operated in negative ion Q3 scan mode (to generate ESI-MS) and product ion mode (to generate ESI-MS/MS). The Q3 scan range was 10-500 m/z and an acquisition time of 0.6 min was used. For the MS/MS experiments, the precursor ion was mass selected with a width of 0.7 amu, and was allowed to undergo collisions with the argon collision gas. The backing pressure of the argon line was 230 kPa, and the pressure inside the collision cell was modelled to be 0.79213 Pa. In these CID experiments, the centre of laboratory collision energies were varied by starting at 10 eV and increasing in 5 eV increments to 40 eV. In tables 1 and 2 the centre of laboratory collision energies are converted to centre of mass collision energies.[8]

2.3 Theoretical Calculations:

All theoretical calculations were performed within the Gaussian 09 program[9] using the M06 functional[10] with all calculations completed in the gas phase. To assess whether the losses of Ph^- and F^- from $PhBF_3^-$ were barrierless, potential energy scans we carried out by stretching the B-C and B-F bonds out to a distance of 4.5 Angstroms using the 6-31+G(d) basis set. Geometry optimizations, frequency calculations and transition state calculations were performed using the large def2-TZVP basis set.[11] The complete model is referred to as M06/def2-TZVP.

3. Results and discussion

3.1 Mass spectrometry

All potassium organotrifluoroborate salts gave abundant organotrifluoroborate anions, RBF_3^-, upon electrospray ionization in the negative ion mode (data not shown). In addition, the alkali metal cluster ions, $K(RBF_3)_2^-$ and $Na(RBF_3)_2^-$ were observed in all cases. The former is expected from a potassium salt, while the latter likely arises from adventitious background sodium cations. In the next sections, we describe the gas-phase fragmentation reactions of RBF_3^-, $K(RBF_3)_2^-$ and $Na(RBF_3)_2^-$ under CID conditions and use DFT calculations to shed light into the energetics of the fragmentation reactions in the cases of R = Me and Ph.

3.1.1 Fragmentation reactions of RBF_3^- under CID conditions

3.1.1.1 R = an alkyl anion, CH_3, CH_3CH_2, $CH_3(CH_2)_3$, $CH_3(CH_2)_5$ and c-C_3H_5.

At lower CID energies, the parent system $MeBF_3^-$ (*m/z* =83) fragments via a single pathway (Figure 1(a)) involving the loss of HF with concomitant formation of the boron stabilized carbanion $CH_2BF_2^-$ (*m/z* =63).[12] Related elimination reactions (eq. 3) have been observed in the fragmentation reactions of Me_3BF^-.[13] At higher collision energies formation of F^- (*m/z* =19) and $CHBF^-$ (*m/z* =43) are also observed (Figure S1) and these are likely to arise from secondary fragmentation reactions of $CH_2BF_2^-$.

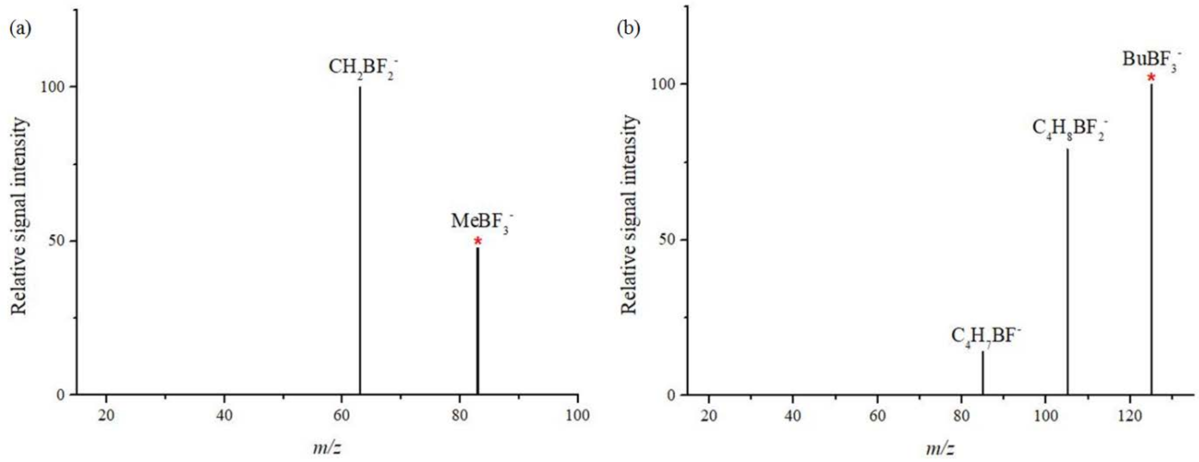

Figure 1: Mass spectra of mass-selected organotrifluoroborate anions and their fragment ions produced upon collision-induced dissociation:

(a) $MeBF_3^-$ (*m/z* 83, collision energy = 20 eV); (b) $BuBF_3^-$ (*m/z* 125, collision energy = 15 eV).

The observed reactivity of $MeBF_3^-$ is consistent with the DFT calculated potential energy diagram (Figure 2) for three potential reactions involving heterolytic cleavage of the B-R or B-F bonds. Cleavage of the B-R bond via barrierless loss of the organic anion, CH_3^- (eq. 1) is the highest energy process, requiring 355.2 kJ/mol and is not observed experimentally. The other two fragmentation processes are associated with cleavage of the B-F bond via loss of F^- (eq.2) and elimination of HF (eq. 3). After initial cleavage of the B-F bond the fluoride anion can either fully depart or can migrate towards the methyl group and abstract a proton resulting in the formation of HF and $CH_2BF_2^-$. The barrier for deprotonation of CH_3BF_2 by F^- (200.8 kJ/mol) lies below the final energy (293.8 kJ/mol) of the separated products of HF elimination, which in turn is lower than the energy for F^- loss, which was calculated at 320.9 kJ/mol. Taken together, these theoretical results are consistent with the fact that HF elimination is the sole fragmentation channel observed under low energy CID conditions. Finally, given the isoelectronic nature of $CH_3BF_3^-$ and CH_3CF_3, it is not surprising that the loss of HF under thermal activation conditions occurs for both species via a cis-1,2 elimination reaction [14,15] and that their calculated mechanisms are similar.[16]

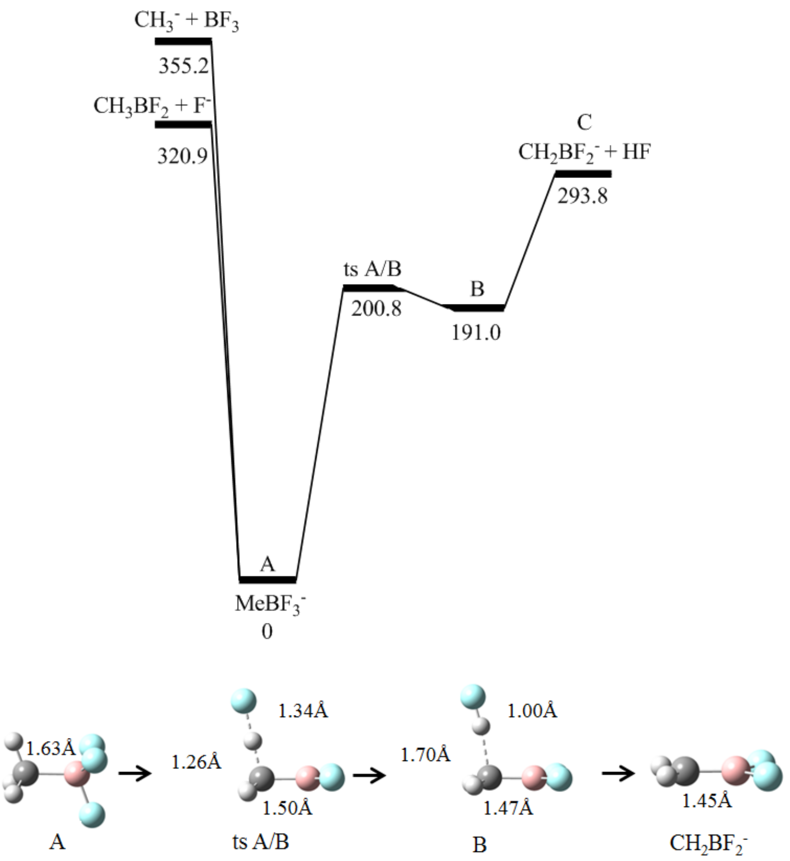

Figure 2: DFT calculated (M06/def2-TZVP) potential energy diagram for $MeBF_3^-$ fragmentation (kJ/mol).

R groups with longer alkyl chains undergo similar losses (Figures S2-S5) as summarized in Table 1 and illustrated for $BuBF_3^-$ (*m/z* =125), which at lower CID energies, also fragments via the loss of HF (Figure 1(b)) resulting in the formation of the boron stabilized carbanion $C_4H_8BF_2^-$ (*m/z* =105). The formation of $C_4H_7BF^-$ (*m/z*=85) is also observed and is the result of a second loss of HF. At higher collision energies formation of F^- (*m/z* =19) and a third loss of HF are also observed (Figure S3).

Table 1: Summary of observed fragmentation pathways from CID experiments on mass selected alkyltrifluoroborate anions.

	Observed fragment ion, centre of mass collision energy where anion first appears in eV and (relative % abundance)			
RBF$_3^-$ (*m/z*)	R$^-$	F$^-$	(R - H)BF$_2^-$	(R - 2H)BF$^-$
MeBF$_3^-$ (83)	(a)	9.8 (7)	3.3 (24)	9.8 (10)
Et BF$_3^-$ (97)	(a)	8.8 (14)	2.9 (31)	(a)
BuBF$_3^-$ (125)	(a)	8.5 (5)	2.4 (77)	2.4 (6)
HexBF$_3^-$ (153)	8.3 (5)	8.3 (7)	2.1 (45)	2.1 (7)
Cyclopropyl BF$_3^-$ (109) (b)	(a)	6.5 (8)	2.7 (13)	8.1 (8)

(a) Channel not observed.
(b) The product ion ($CH_2BF_2^-$, *m/z* =63) is also observed at a centre of mass collision energy of 6.7 eV with a relative abundance of 30%.

3.1.1.2 R = the stabilised anions, C_6H_5, $C_6H_5CH_2$, CH_2CHCH_2, CH_2CH and C_6H_5CO.

At lower CID energies, PhBF$_3^-$ (*m/z* =145) fragments via a single pathway (Figure 3(a)). However, in contrast to the alkyl anions this fragmentation occurs via cleavage of the R-B bond to form the phenyl anion (*m/z* =77, eq. 1). At higher collision energies, the formation of F$^-$ (*m/z* =19) is also observed (Figure S9). For the fragmentation of PhBF$_3^-$ two possible pathways were considered; the elimination of $C_6H_5^-$ (eq. 1) and the elimination of F$^-$ (eq. 2) (Figure 3). The elimination of $C_6H_5^-$ was determined to be barrierless based upon a potential energy scan in which the B-C bond of PhBF$_3^-$ was stretched. No inflection points were observed (Figure S6), and attempts to optimize a transition state using the structure optimized at 3.3 Ansgtroms from this scan resulted in the two fragments continuing to migrate away from each other and ultimately failed. In PhBF$_3^-$ the three fluorine atoms are found in two different environments; one lies in the plane of the phenyl ring whilst the other two related by symmetry are positioned above and below the plane of the ring. Scans lengthening the B-F bond from these two environments showed small inflection points (Figures S7 and S8). Transition state calculations performed on each of these points produced identical transition states in which the eliminated fluorine anion forms a hydrogen bond to the closest hydrogen atom of the phenyl ring. The barrier for this transition state (243.9 kJ/mol) lies below the final energy for F^- elimination (309.2 kJ/mol). The relative energies of the $C_6H_5^-$ and fluoride elimination pathways were 309.2 and 345.1 kJ/mol respectively indicating that $C_6H_5^-$ elimination should be the favoured pathway. These computational results (Figure 4) are in agreement with the experimental spectra where the only product observed at lower energies is the $C_6H_5^-$ anion (Figure 3(a)).

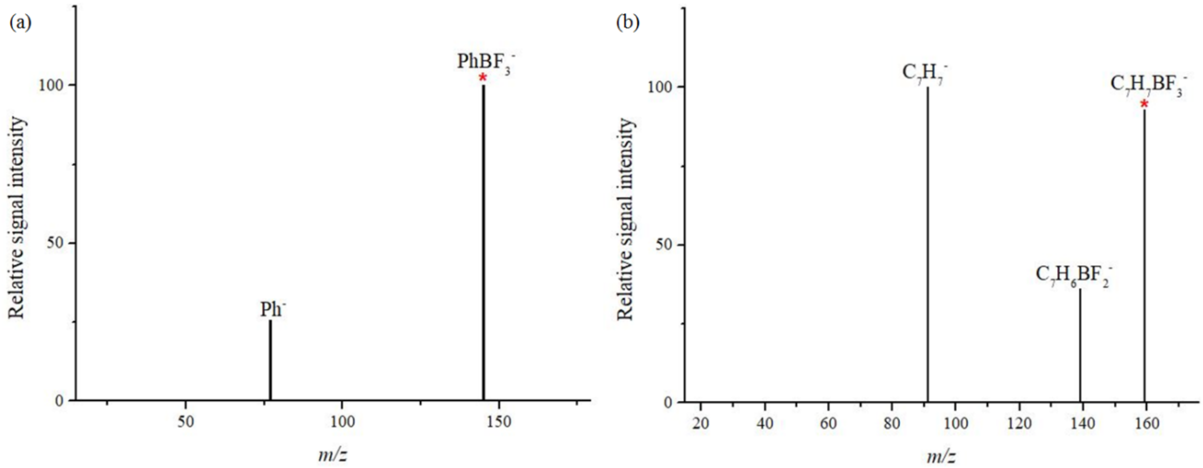

Figure 3: Mass spectra of mass-selected organotrifluoroborate anions and their fragment ions produced upon collision-induced dissociation: (a) $PhBF_3^-$ (*m/z* 145, collision energy = 15 eV); (b) benzyl BF_3^- (*m/z* 159, collision energy = 20 eV).

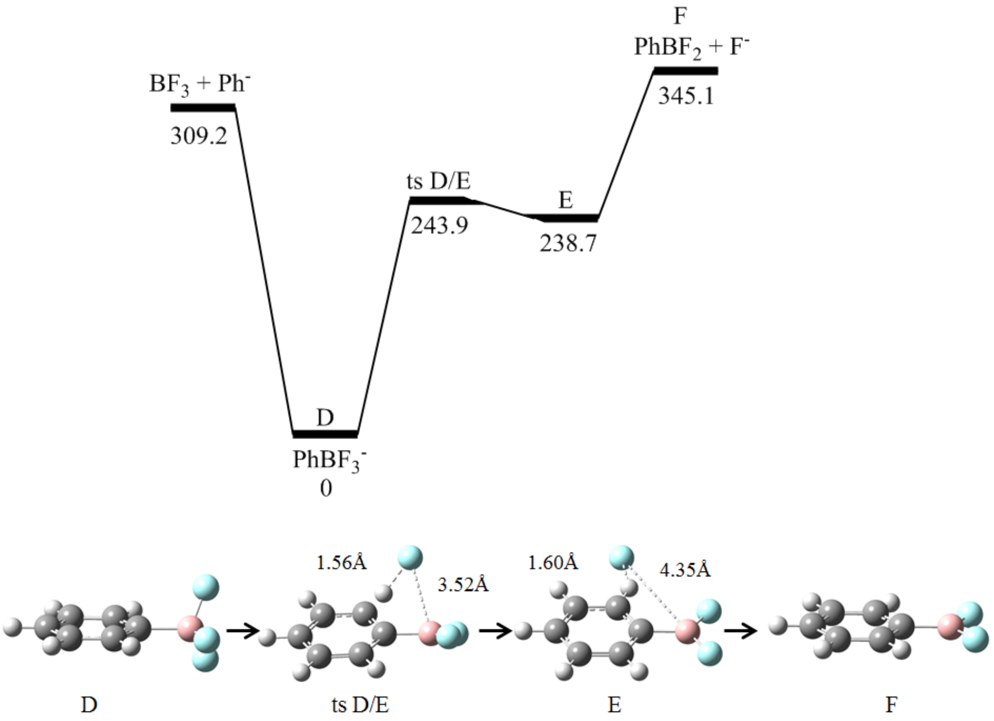

Figure 4: DFT calculated (M06/def2-TZVP) potential energy diagram for $PhBF_3^-$ fragmentation (kJ/mol).

At lower CID energies, benzylBF_3^- (*m/z* =159) also fragments via the loss of R^- producing the $C_7H_7^-$ ion (*m/z* =91) (Figure 3(b)). In addition to this pathway it can also fragment via the loss of HF to form $C_7H_6BF_2^-$ (*m/z* =139), a reaction similar to that discussed for $MeBF_3^-$ above. At higher collision energies the formation of $C_7H_5BF^-$ (*m/z* =119) from a secondary HF loss is also observed (Figure S10).

In contrast to the other studied stabilised anions the allyltrifluoroborate anion (*m/z* =109) does not fragment (Figure S11) via the loss of R^- (eq. 1) and at lower collision energies the sole fragmentation pathway is the elimination of HF forming the $C_3H_4BF_2^-$ ion

(m/z=89, eq. 3). At higher collision energies release of F^- (eq. 2) is observed in addition to the formation of $CH_2BF_2^-$ (m/z=63) and $C_3H_3^-$ (m/z=39).

The vinyltrifluoroborate anion (m/z=95) fragments (Figure S12) primarily via the loss of R^- (eq. 1). It also fragments via loss of F^- (eq. 2) and elimination of HF (eq. 3). Initial fragmentation of the vinyl BF_3^- (m/z=95) occurs at a higher collision energy than any of the other studied systems. Thus, an examination of Table 2 reveals that initial fragmentation occurs at a centre of mass collision energy of 1.9-2.7 eV for all systems apart from the vinyltrifluoroborate anion for which ions do not appear until a centre of mass collision energy of 5.9 eV.

Table 2: Summary of observed fragmentation pathways from CID experiments on mass selected organotrifluoroborate anions, RBF_3^-, where R = a stabilised anion.

	Observed fragment ion, centre of mass collision energy where anion first appears in eV and (relative % abundance)			
RBF_3^- (m/z) EA [(a)]	R^-	F^-	$(R - H)BF_2^-$	$(R - 2H)BF^-$
PhBF_3^- (145) 1.096	2.2 (78)	7.6 (9)	(b)	(b)
benzyl BF_3^- (159) 0.912	2.0 (88)	(b)	2.0 (22)	6.0 (10)
allyl BF_3^- (109) 0.481[(c)]	(b)	10.7 (9)	2.7 (49)	(b)
vinyl BF_3^- (95) 0.667	7.4 (69)	7.4 (12)	5.9 (8)	(b)
benzoyl BF_3^- (173) 0.56 [(d)]	(b)	(b)	(b)	(b)

(a) EA = electron affinity in eV, taken from ref 19b.
(b) Channel not observed.
(c) The product ion $CH_2BF_2^-$ (m/z=63) is also observed at a centre of mass collision energy of 5.4 eV with a relative abundance of 18%.

(d) The product ion Ph^- (*m/z* =77) also observed at a centre of mass collision energy of 1.9 eV with a relative abundance of 26%.

At all studied collision energies, the sole product upon CID of benzoyl BF_3^- is the Ph^- (*m/z* =77) ion formed via loss of CO and BF_3 from the parent benzyltrifluoroborate anion (*m/z* =173) (Figure S13). This ion might be formed via either of two pathways: concerted loss of CO and BF_3 (eq. 6); or initial loss of BF_3 to produce the benzoyl ion (*m/z* =105, eq. 7), which then loses CO to produce the Ph^- ion (*m/z* =77, eq. 8). Since acyl anions are stable species in the gas-phase[17,18] and the benzoyl ion is not observed in our experiments, its seems likely that the concerted pathway operates.

$$(C_6H_5CO)BF_3^- \rightarrow C_6H_5^- + BF_3 + CO \quad (6)$$

$$(C_6H_5CO)BF_3^- \rightarrow C_6H_5CO^- + BF_3 \quad (7)$$

$$C_6H_5CO^- \rightarrow C_6H_5^- + CO \quad (8)$$

3.1.2 Fragmentation reactions of $K(RBF_3)_2^-$ and $Na(RBF_3)_2^-$ under CID conditions.

In addition to the bare organotrifluoroborate anions, $M(RBF_3)_2^-$ clusters (where M = Na and K) were observed in the ESI-MS of all potassium organotrifluoroborate salts. These alkali metal clusters can undergo fragmentation via two competing pathways; formation of RBF_3^- (eq. 4) or fluoride transfer (eq. 5). In each of the spectra of clusters shown in Figure 5 the formation of RBF_3^- was favoured over fluoride transfer regardless of whether the R group was methyl or phenyl.

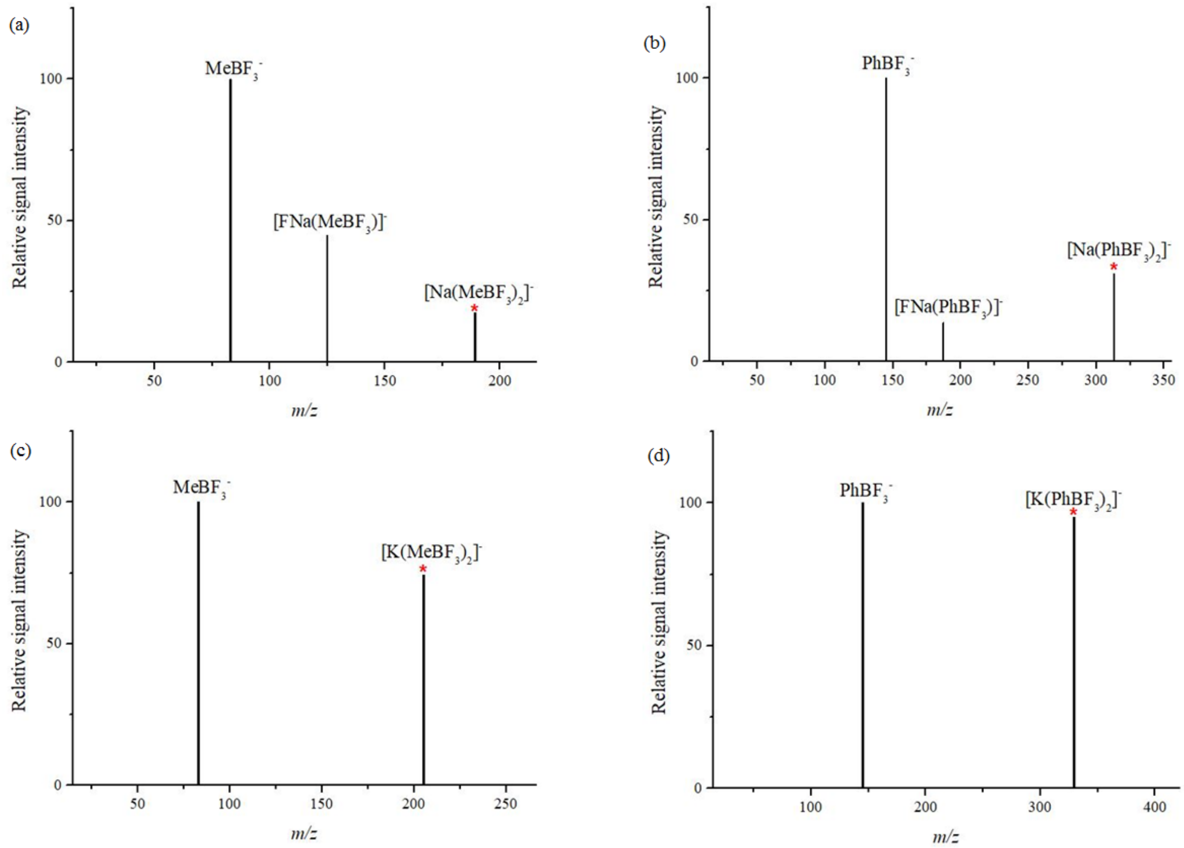

Figure 5: Mass spectra of mass-selected anions and their fragment ions produced upon collision-induced dissociation: (a) $Na(MeBF_3)_2^{-}$ (*m/z* 187, collision energy = 15 eV); (b) $Na(PhBF_3)_2^{-}$ (*m/z* 313, collision energy = 15 eV); (c) $K(MeBF_3)_2^{-}$ (*m/z* 203, collision energy = 10 eV); (d) $K(PhBF_3)_2^{-}$ (*m/z* 329, collision energy = 10 eV).

The nature of the alkali metal influences whether fluoride transfer occurs (eq. 5). Thus fluoride transfer is observed in the CID spectra of $Na(MeBF_3)_2^{-}$ and $Na(PhBF_3)_2^{-}$ (Figures 5(a) and (b)), with a greater proportion of fluoride transfer occurring in the methyl complex than the phenyl. In contrast, fluoride transfer was wholly absent in the CID spectra of $K(MeBF_3)_2^{-}$ and $K(PhBF_3)_2^{-}$ (Figures 5(c) and (d)). This trend of fluoride transfer occurring upon CID of $Na(RBF_3)_2^{-}$ but not for $K(RBF_3)_2^{-}$ was maintained across all of the studied systems (Table 3).

Table 3: Summary of observed fragmentation pathways from CID experiments on mass selected $M(RBF_3)_2^-$ anions.

	Relative % abundance of fluoride transfer and formation of RBF_3^-			
R	$Na(RBF_3)_2^-$ (10 eV)		$K(RBF_3)_2^-$ (15 eV)	
	$FNa(RBF_3)^-$	RBF_3^-	$FK(RBF_3)^-$	RBF_3^-
Me	37	52	0	100
Et	55	89	0	100
Bu	55	94	0	100
Hex	19	36	0	100
cyclopropyl	45	81	0	100
Ph	8	92	0	100
benzyl	0	85	0	100
allyl	14	100	0	100
vin	24	91	0	100
benzoyl	0	88	0	100

Although the fluoride anion affinities of the neutral salts $M(RBF_3)$ (M = Na and K, R = Me and Ph) are unknown, using the known gas-phase heats of formation of Na^+ (603.1 kJ/mol), K^+ (507.8 kJ/mol), F^- (249 kJ/mol), NaF (-290.5 kJ/mol), and KF (-326.8 kJ/mol),[19] the higher fluoride anion affinity of Na^+ (1142.6 kJ/mol) is calculated to be higher than that of K^+ (1083.6 kJ/mol). Thus, the experimentally observed preference for fluoride transfer from RBF_3^- to $Na(RBF_3)$ is consistent with the higher fluoride anion affinity of Na^+. To confirm that $Na(RBF_3)$ had a higher fluoride anion affinity than $K(RBF_3)$ and to compare the reaction energetics associated with the competition between release of RBF_3^- (eq. 4) and fluoride transfer (eq. 5), DFT calculations were carried out for

$Na(RBF_3)_2^-$ and $K(RBF_3)_2^-$ (where R = Me and Ph) and the results are summarized in Table 4.

Table 4: Relative energies for fragmentation of alkali metal clusters (kJ/mol) (M06/def2-TZVP): (a) $Na(MeBF_3)_2^-$; (b) $Na(PhBF_3)_2^-$; (c) $K(MeBF_3)_2^-$; (d) $K(PhBF_3)_2^-$.

Cluster	Relative energy of formation of RBF_3^- (eq. 4)	Relative energy of F^- transfer (eq. 5)	Energy difference between eq. 4 and 5
$Na(MeBF_3)_2^-$	181.7	192.1	10.4
$Na(PhBF_3)_2^-$	170.2	182.2	12.0
$K(MeBF_3)_2^-$	175.1	216.3	41.2
$K(PhBF_3)_2^-$	157.4	200.9	43.5

For the sodium metal clusters $Na(MeBF_3)_2^-$ and $Na(PhBF_3)_2^-$ it was found that the release of RBF_3^- (R=Me, Ph) is thermodynamically favoured over fluoride transfer in both cases by 10.4 and 12.0 kJ/mol respectively (Table 4). These results are in agreement with the experimental spectra which show RBF_3^- as the major product after CID of $Na(MeBF_3)_2^-$ and $Na(PhBF_3)_2^-$ with only a small proportion of fluoride transfer observed.

The same trend is observed for $K(MeBF_3)_2^-$ and $K(PhBF_3)_2^-$, with RBF_3^- release favoured over fluoride transfer by 41.2 and 43.5kJ/mol. These trends are consistent with the experimental spectra where fluoride transfer is solely observed in the sodium clusters with the energy gap between the between formation of RBF_3^- and fluoride transfer being much larger in the potassium clusters than their sodium counterparts.

4. Conclusions

Negative ion electrospray ionization of potassium organotrifluoroborates salts produces abundant organotrifluoroborate anions, RBF_3^-, together with the alkali metal cluster ions, $K(RBF_3)_2^-$ and $Na(RBF_3)_2^-$. The preferred fragmentation pathway of RBF_3^- ions upon CID depends on the nature of the R group, with alkyl systems fragmenting via loss of HF to generate boron stabilized anions (eq. 3), while systems which can release a stabilised anion, R^- (where electron affinity of the conjugate radical is > 0.56 eV) generally fragmenting via the loss of BF_3 (eq. 1, Table 2). This preference is confirmed by DFT calculations on the fragmentation pathway of $MeBF_3^-$ and $PhBF_3^-$ ions.

The loss of HF generates boron stabilized carbanions (eq. 3) which are isoelectronic with alkenes. Related losses from other organoboron anions have been noted to generate interesting boron-containing species that are isoelectronic with a range of neutral carbon analogues such as allene and ketene.[13,20]

In contrast to the fragmentation reactions of organomagnesate anions[21,22], organozincate[23], organoferrate[24], organoindates [25] and coinage metal organometallate anions[26-30], reductive elimination, beta hydride transfer reactions and bond homolysis reactions that release radicals are not observed for organotrifluoroborate anions, RBF_3^-.

The preferred fragmentation pathway for $K(RBF_3)_2^-$ and $Na(RBF_3)_2^-$ involves formation of RBF_3^- (eq. 4). While $Na(RBF_3)_2^-$ also undergoes a minor amount of fluoride anion transfer (eq. 5), this pathway does not operate for $K(RBF_3)_2^-$, consistent with the known relative fluoride anion affinities of Na^+ and K^+ and with DFT calculations of the energetics of fragmentation of $K(RBF_3)_2^-$ and $Na(RBF_3)_2^-$ (where R = Me and Ph). These differences in the fluoride ion transfer reactions can be rationalized by Pearson's HSAB theory,[31] where the hard base F$^-$ prefers reacting with the harder Na$^+$ acid.[32]

5. Acknowledgements

We thank the Australian Research Council for financial support (DP180101187). The DFT calculations were carried out using: (i) the National Computing Infrastructure – we thank Prof. Allan J. Canty for access; (ii) University of Melbourne (2017) Spartan HPC-Cloud Hybrid.[33]

6. References

(1) Fernández E, Whiting A. Eds. Synthesis and Application of Organoboron Compounds. *Top Organomet Chem* 2015; 49.

(2) Hall DG, ed. *Boronic Acids: Preparation, Applications in Organic Synthesis and Medicine*. 2nd ed. Weinheim, Germany: WILEY-VCH; 2011.

(3) Molander GA. Organotrifluoroborates: Another Branch of the Mighty Oak. *J Org Chem* 2015; 80: 7837–7848.

(4) Darses S, Genet JP. Potassium organotrifluoroborates: new perspectives in organic synthesis. *Chem Rev* 2008; 108: 288-325.

(5) Darses S, Genet JP. Potassium Trifluoro(organo)borates: New Perspectives in Organic Chemistry. *Eur J Org Chem* 2003; 4313–4327.

(6) Petrillo DE, Kohli RK, Molander GA. Accurate mass determination of organotrifluoroborates. *J Am Soc Mass Spectrom* 2007; 18: 404-405.

(7) Churches QI, Hooper JF, Hutton CA. A General Method for Interconversion of Boronic Acid Protecting Groups: Trifluoroborates as Common Intermediates. *J Org Chem* 2015; 80: 5428-5435.

(8) Douglas DJ. Applications of Collision Dynamics in Quadrupole Mass Spectrometry, *J Am Soc Mass Spectrom* 1998; 9: 101–113.

(9) Frisch MJ, et al. Gaussian_09, Revision D.01; Wallingford, CT: Gaussian, Inc; 2013.

(10) Zhao Y, Truhlar DG. The M06 suite of density functionals for main group thermochemistry, thermochemical kinetics, noncovalent interactions, excited states, and transition elements: two new functionals and systematic testing of four M06-class functionals and 12 other functionals. *Theor Chem Acc* 2008; 120: 215-241.

(11) Weigend F, Ahlrichs R. Balanced basis sets of split valence, triple zeta valence and quadruple zeta valence quality for H to Rn: Design and assessment of accuracy. *Phys Chem Chem Phys* 2005; 7: 3297-3305.

(12) Olmstead MM, Power PP, Weese KJ, Doedens RJ, Isolation and X-ray crystal structure of the boron methylidenide ion $[Mes_2BCH_2]^-$ (Mes = 2,4,6-$Me_3C_6H_2$)—a boron–carbon double bonded alkene analogue. *J Am Chem Soc* 1987; 109: 2541-2542.

(13) Oomens J, Steill JD, Morton TH. IR Spectra of Boron-Stabilized Anions in the Gas Phase. *Inorg Chem* 2010; 49: 6781-6783.

(14) DePuy CH, King RW. Pyrolytic Cis Eliminations. *Chem Rev* 1960; 60: 431–457

(15) Tsang W, Lifshitz A. Kinetic stability of 1,1,1-Trifluoroethane. *Int J Chem Kin* 1998; 30: 621-628.

(16) Dubnikova F, Lifshitz A. Formation of Van Der Waals Complexes in Concerted Unimolecular Elimination Processes. *ISRN Phys Chem* 2012, Article ID 431367, 7 pages, doi:10.5402/2012/431367.

(17) DePuy CH, Bierbaum VM, Damrauer R, Soderquist JA. Gas-phase reactions of the acetyl anion. *J Am Chem Soc* 1985; 107: 3385–3386.

(18) Kleingeld JC, Nibbering NMM. A fourier transform ion cyclotron resonance study of the gas phase negative ion chemistry of benzaldehyde. *Tetrahedron* 1984; 40: 2789-2794.

(19) Thermochemical data for heats of formation are from: (a) Lias SG, Bartmess JE, Liebman JF, Holmes JL, Levin RD, and Mallard WG. Gas-Phase Ion and Neutral Thermochemistry. *J Phys Chem Ref Data* 1988;

17(1); (b) Burgess DR. Thermochemical Data In: Linstrom PJ, Mallard WG, ed. *NIST Chemistry WebBook, NIST Standard Reference Database Number 69*, Gaithersburg, MD, National Institute of Standards and Technology; 20899, doi:10.18434/T4D303, (retrieved January 29, 2018).

(20) Sheldon JC, Currie GJ, Bowie JH. Bismethyleneborane $[B(CH_2)_2]^-$ and trismethyleneborane $[B(CH_2)_3]^-$ anions. Do they exist in the gas phase? *J Am Chem Soc* 1988; 110: 8266–8267.

(21) Thum CCL, Khairallah GN, O'Hair RAJ, R. Gas-Phase Formation of the Gomberg-Bachmann Magnesium Ketyl. *Angew Chem Int Ed* 2008; 48: 9118.

(22) Khairallah GN, Thum CCL, Lesage D, Tabet JC, O'Hair RAJ. Gas-Phase Formation and Fragmentation Reactions of the Organomagnesates, $[RMgX_2]^-$. *Organometallics* 2013; 32: 2319.

(23) Koszinowski K, Böhrer P. Aggregation and Reactivity of Organozincate Anions Probed by Electrospray Mass Spectrometry. *Organometallics* 2009; 28: 100-110.

(24) Parchomyk T, Koszinowski K. Ate Complexes in Iron-Catalyzed Cross-Coupling Reactions. *Chem Eur J* 2016; 22: 15609 – 15613.

(25) Koszinowski K. Oxidation State, Aggregation, and Heterolytic Dissociation of Allyl Indium Reagents. *J Am Chem Soc* 2010; 132: 6032–6040.

(26) Rijs NJ, Yates BF, O'Hair RAJ. Dimethylcuprate undergoes a dyotropic rearrangement. *Chem Eur J* 2010; 16: 2674 – 2678.

(27) Rijs NJ, O'Hair RAJ. Unimolecular Reactions of Organocuprates and Organoargenates. *Organometallics* 2010; 29: 2282 – 2291.

(28) Putau A, Koszinowski K. Probing Cyanocuprates by Electrospray Ionization Mass Spectrometry. *Organometallics* 2010; 29: 3593–3601.

(29) Rijs NJ, Sanvido GB, Khairallah GN, O'Hair RAJ. Gas phase synthesis and reactivity of dimethylaurate. *Dalton Trans* 2010; 39: 8655.

(30) Kolter M, Koszinowski K. Stability and Unimolecular Reactivity of Palladate(II) Complexes [LnPdR3](-) (L=Phosphine, R=Organyl, n=0 and 1). *Chem Eur J* 2016; 22: 15744-15750.

(31) Pearson RG. Hard and Soft Acids and Bases. *J Am Chem Soc* 1963; 85: 3533–3539.

(32) Parr RG, Pearson RG. Absolute hardness: companion parameter to absolute electronegativity. *J Am Chem Soc* 1983; 105: 7512–7516.

(33) Meade B, Lafayette L, Sauter G, Tosello D. Spartan HPC-Cloud Hybrid: Delivering Performance and Flexibility. University of Melbourne. 2017, https://doi.org/10.4225/49/58ead90dceaaa.